FUDMA Journal of Renewable and Atomic Energy (FJoRAE)
ISSN: 3027-2335
Vol. 1 No 1, March 2024. Pp 61-76

https://doi.org/10.33003/fjorae-2024-0101.06

Effect of High Concentration of Equivalent Thorium (eTh) And Uranium (eU) Within Part of North Central Nigeria on Geothermal Parameters

Adetona A. Adebayo[1*], Kwaghhua I. Fidelis[2], Aisha Alkali[3]

[1, 2, 3] Federal University of Technology Minna, Niger State, Nigeria.
*** Corresponding author's email**: fidelisik@gmail.com, a.abbass@futminna.edu.ng[2], aisha.alkali@futminna.edu.ng[3]

Abstract

A high amount of heat flow from a shallow curie depth is essentially related to a promising geothermal resource. This work explores the depth of demagnetisation due to high radiogenic heat content of the basement rocks. The Total Magnetic Intensity and the radiometric data, consisting of the Potassium count, the Uranium and Thorium equivalents, were employed for the research work. Sheet 145 (Kajuru) and 146 (Geshere) both on latitude 10°00'N to 10°30'N and longitude 7°30'E to 8°30'E covering 6,050 km^2 within Kaduna State of Central Nigeria is an area with notedly high concentrations of these radionuclide by previous researchers. A shallow Curie point depth of 12.00 km was observed below Wugana while heat flow values ranging from 30.00 mW/m^2 to 160 mW/m^2 was estimated with an average of 80.60 mW/m^2. Also, the geothermal gradients varied from 8.00 to 50.00 °CKm^{-1}, with an average value of 25.50 °CKm-1. The effect of heat generated from the Potassium count, equivalent concentrations of Uranium and Thorium indicated the Northern end down to the Mid-western end displays medium to high radiogenic heat production (3.6 – 4.5 μW/m^3). In conclusion, areas with low Currie depth that coincide with relatively high radiogenic heat production are located within Wugana, New Kwasan, and down to Ron villages, which are generally located at the Mid-North and Mid-Western areas with intrusive granitic rocks

Keywords: Curie depth, Geothermal, Heat Flow, Aeromagnetic and radiometric data

1. Introduction

Geothermal energy is associated with heat produced as a result of radioactive processes from either Potassium (K), equivalent Uranium (eU) or Thorium (eTh) within the earth crust. This form of energy is in-exhaustible, environmentally friendly and globally available for electrical energy production and other industrial uses (Mock et al., 1997; Rybach, 2010; McCay et al., 2014; Younger, 2015). The essential geothermal parameters and indicators for assessing a viable potential geothermal energy source or reservoir are the Curie point depth, geothermal gradient and heat flow (Jessop et al., 1976; Cull and Conley, 1983; Okubo et al., 1985; Obande et al., 2014; Nwankwo and Shehu, 2015). In regions of the earth crust where decayed radio nuclide particles generate enough heat that converts the magnetic susceptibility of the rock to zero, this will lead to shallow curie

depth and high heat flow that can be harnessed for various usage of economic importance (Adetona et al., 2024; Adetona et al., 2023; McCay et al., 2014; Olorunsola and Aigbogun, 2017; Abdel Zaher et al., 2018a; Akinnubi and Adetona, 2018; Salako et al, 2020). Two factors that could lead to such scenario (high radiogenic heat production) are concentration and degree of decay of radio nuclei particle in the basement rock.

Gamma-ray spectrometric survey have been identified as a means of accurately determining the crustal concentrations of the three radiogenic elements simultaneously (Brookins, 1982; Chiozzi et al., 2003). There has been a review of the radio nuclei concentration of Nigeria from the radiometric data of the country as compiled by Nigeria Geological Survey Agency in the year 2009 to 2011. The review presented in mappings showed high concentration of radioelements within parts of north central Nigeria. Also, the existence of relatively high concentration of both uranium and thorium within the young granite of Plateau and Kaduna States at certain areas like, Kajuru, Kachia, Naraguta and Maijuju was also reported in some ground truthing exploration by other researchers such as (Atipo and Olarinoye, 2020; Arisekola, 2020). This concentration is expected to affect the heat content within the lithology. Hence, the attention of researchers is drawn to the area

The primary aim of this research is to investigate the effect of high concentration of equivalent Thorium (eTh) and equivalent Uranium (eU) radio nuclides observed on sheets 145 (Kajuru) and 146 (Geshere) on the curie point depth, and subsequently, geothermal gradient and heat flow values within the study area. While spectral analysis of the airborne magnetic data will be used to assess the geothermal parameters (Curie point, thermal gradient and heat flow); a measure of concentration of radioelements will be used to determine the radiogenic heat production. A comparison of these analysis will show the effect and contribution of high concentration of radioelements to the geothermal nature of study area.

2. Location and geology of the study area

The location of study spans a total area of 6,050 km^2 and is enclosed within latitude 10°00' to 10°30'N and longitude 7°30' to 8°30'E in Kaduna State North Central Nigeria. Map of the study area Figure 1, indicates the area falls within sheet 145 (Kajuru) and 146 (Geshere) respectively. Major towns within the study area include Kujama, Kajuru, Idom, Doka and Kaduna which is the state capital. Geological formations within the area (Figure 2) includes Young Basalt, Biotite Granite, Amphibolite Schist, Migmatite and other undifferentiated grades of Granites.

ISSN: 3027-2335 https://fjorae.fudutsinma.edu.ng

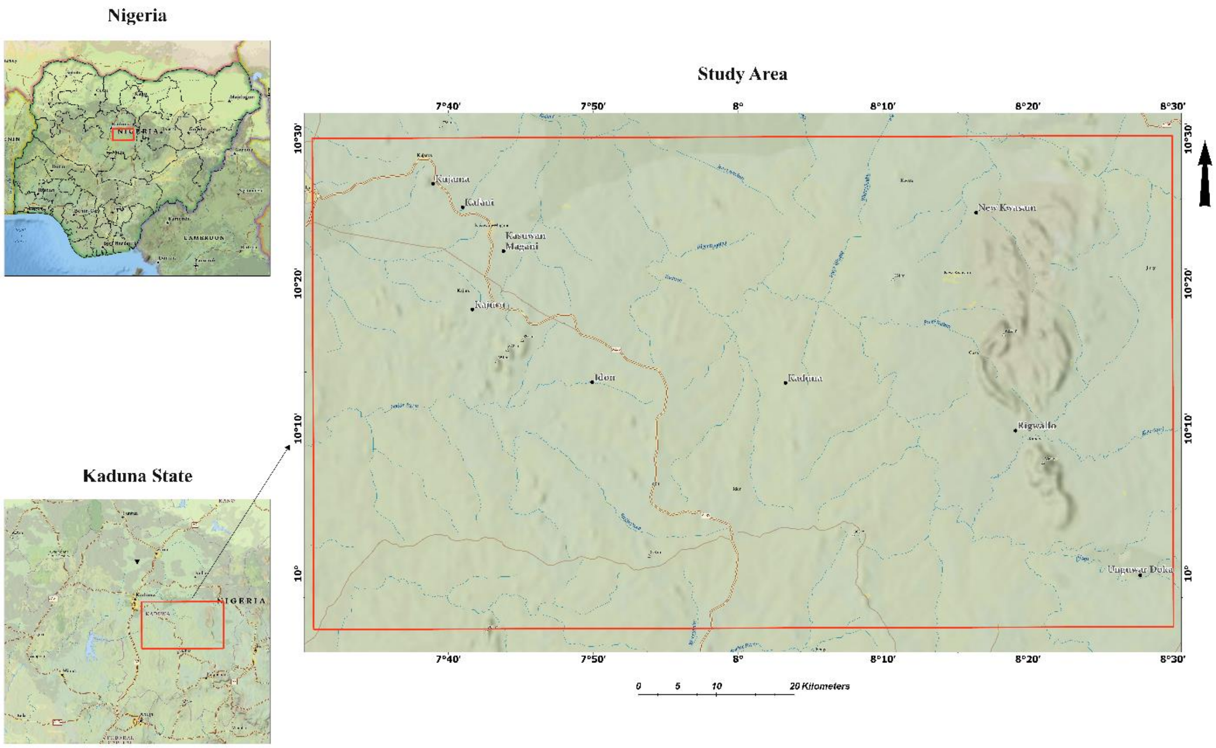

Figure 1: Location map of study area

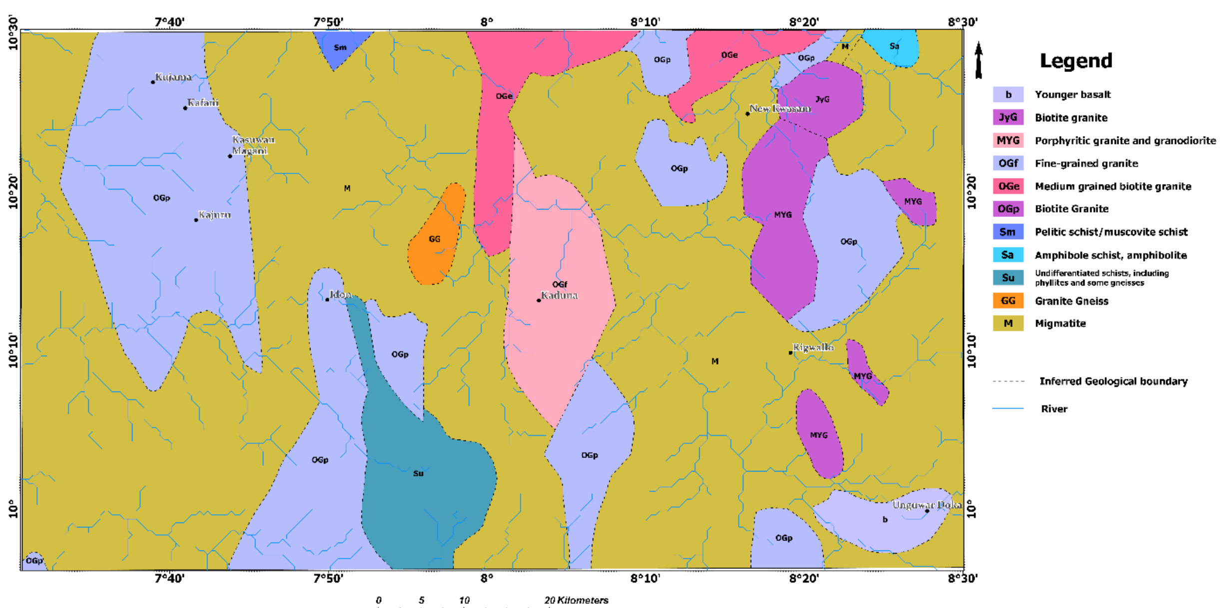

Figure 2: Geology map of the study area (Modified from NGSA, 2009).

ISSN: 3027-2335 https://fjorae.fudutsinma.edu.ng

3. Materials and Methods

3.1 Data source and specifications

Both the Aero-magnetic and Aero-radiometric data that covered the study area was obtained from Nigeria Geological Survey Agency (NGSA). The data acquisition was carried by Fugro Airborne Survey in 2009 using Cessna Caravan 208B ZS-FSA and Cessna Caravan 208 ZS-MSJ aircrafts, 3 x Scintrex CS3 Cesium Vapour magnetometer, for magnetic data, 512-channels gamma-ray spectrometer, a NaI(TI) crystals mounted on fixed-wing aircraft for the radiometric data. Other specifications include, 5000- and 2000-meters Tie Line Spacing for the magnetic and radiometric data respectively, 500 meters Flight Line Spacing, 80 meters Sensor Mean Terrain Clearance and 0.1 seconds or less Recording Interval for both data sets. The flight line direction was NW–SE (135°), and the control line was in NE–SW direction (45°).

3.2 Theory of Methods

3.2.1 Spectral Depth Analysis

The algorithm for the models of the centroid method employed the shape of an isolated magnetic anomaly, by Bhattacharyya and Leu (1975, 1977) and applied to the statistical properties of magnetic ensembles by Spector and Grant (1970). Blakely (1995) extended the same to power spectral density of magnetic field, $\phi\Delta T(k_x, k_y)$as:

$$\phi\Delta T(k_x, k_y) = \phi_M(k_x, k_y).4\pi^2 {C_M}^2 |\Theta_M|^2 |\Theta_f|^2 e^{-2|k|Z_t}\left(1 - e^{-2|k|(Z_b - Z_t)}\right)^2 \quad (1)$$

$$\varphi\Delta\beta(C_x, C_y) = \varphi_M(C_x, C_y).4\pi^2 {K_M}^2 |\sigma_M|^2 |\sigma_f|^2 e^{-2|c|z_t}\left(1 - e^{-2|c|(z_b - z_t)}\right)^2$$

C_x and C_y are wave numbers in cartesian coordinate , $\varphi_M(C_x, C_y)$ spectral of magnetization, K_M is a constant, φ_M and φ_f are magnetization and field direction, and z_b and z_t are depths to magnetic basement and of overburden layer respectively.

If the layer's magnetization is random function in x, y it implies that $\varphi_M(C_x, C_y)$is a constant, and therefore the azimuthally averaged power spectrum, $\varphi(|C|)$would be given as

$$\varphi(|C|) = Ae^{-2|c|z_t}\left(1 - e^{-2|C|(z_b - z_t)}\right)^2 \quad (2)$$

3.2.2 Depth to the Top (z_t), Centroid (z_0) and Bottom (z_b) of Magnetic sources

Two approaches were involved here,

1. Depth of the overburden is obtained from the slope of the high-wave-number portion of the power spectrum as:

$$\ln\left(P\left((k)^{\frac{1}{2}}\right) = A - |k|z_t \quad (3)$$

where$P(k)$ is the azimuthally averaged power spectrum, k is the wave number $(2\boldsymbol{\pi}\ \boldsymbol{k}m^{-1}), A$ is a constant, and Z_t is the depth to the top of magnetic sources.

2. The centroid depth, which comprise of both the overburden and the basement rocks is obtained from the low-wave-number portion as, (Tanaka *et al.*, 1999)

ISSN: 3027-2335 https://fjorae.fudutsinma.edu.ng

$$\ln\left(P\left((k)^{\frac{1}{2}}/k\right)\right) = B - |k|z_0 \quad (4)$$

if B is a constant then z_0 is the centroid.

The depth to magnetic source (Z_b) that has a constant density and Thermal conductivity of 2.5W/m/°C for granite required for evaluating the Geothermal Gradient is obtained from the relation (Okubo *et al.,* 1985 Adetona *et al.*,2017):

$$Z_b = 2Z_0 - Z_t \quad (5)$$

3.2.3 Geothermal Gradient and Heat Flow

Using the result of (Z_b), in equation 5 above, the geothermal gradient $\left(\frac{dT}{dZ}\right)$ can be estimated as:

$$\left(\frac{dT}{dZ}\right) = \left(\frac{\Theta_c}{Z_b}\right) \quad (6)$$

Where Θ_c is the Curie temperature.

By employing, Z_b and $\frac{dT}{dZ}$, the heat flow (q_z) can be estimated as (Okubo *et al.,* 1985):

$$q_z = -\sigma\left(\frac{\Theta_c}{Z_b}\right) = -\sigma\left(\frac{dT}{dZ}\right), \quad (7)$$

Where σ is thermal Conductivity, a value of 2.5W/m/°C is the average for igneous rocks at a Curie temperature of 580 °C (Stacey, 1977; Trifonova *et al.,* 2009).

3.2.4 Spectral Analysis Procedure

i. In order to estimate the Curie point depth, geothermal gradient and heat flow, the TMI map was divided into nine sub-sheets for spectral analysis.
ii. Each sub-sheet was further subjected to Fast Fourier Transform, a process which decomposes the magnetic values to its energy spectrum and wave number components.
iii. The data from spectral analysis was used to calculate depth to the top and centroid of magnetic sources. The obtained depths were then used to calculate the Curie point depth (CPD) using equation (5). The CPD values were used to estimate the heat flow and geothermal gradient using equations (6) and (7), respectively.

3.3 Radiogenic Heat Production Procedure

The concentration of the three radio elements (K, eTh, and eU) was used to calculate the radiogenic heat production of rocks in the study area from an empirical equation given by Rybach (1976).

$$A(\mu W/m^3) = \rho(0.0952C_U + 0.0256C_{Th} + 0.0348C_K) \quad (8)$$

where: ρ is rock density (kg m^{-3}), C_K is the concentration of potassium by percentage weight, Cu and C_{Th} are the concentrations of uranium and thorium in ppm. A numerical constant is multiplied by each radioelement concentration. The constants indicate the various contributions made by each radioelement to radiogenic heat generation. The constant for uranium (0.097) is more than twice the constants for potassium (0.035) or

ISSN: 3027-2335 https://fjorae.fudutsinma.edu.ng

thorium (0.026), indicating that uranium dominates thorium and potassium in terms of heat production. (Bücker and Rybach, 1996; McCay *et al.,* 2014). Also, the density values were a reflection of average densities of rocks types hosting the radioelements with in the area of study (Adetona *et al.,* 2024; Madu *et al.*, 2015; Olorunsola and Aigbogun, 2017; Telford *et al.,* 1990).

4. Results and Discussion

4.1 Results and Interpretation of Magnetic Signatures within the Study Area

The residual magnetic intensity map Figure (3), comprises both positive and negative anomalies and ranges from -145.062 nT to 47.293 nT. The deep blue to pink colours on the map represents the range of magnetic intensity from low to high. It reveals various degrees of high magnetic susceptibility in the left-hand part of the study area, while low magnetic susceptibility occupies the south eastern part of the study area. The map was divided into nine sub-sheets for spectral analysis pre-processing.

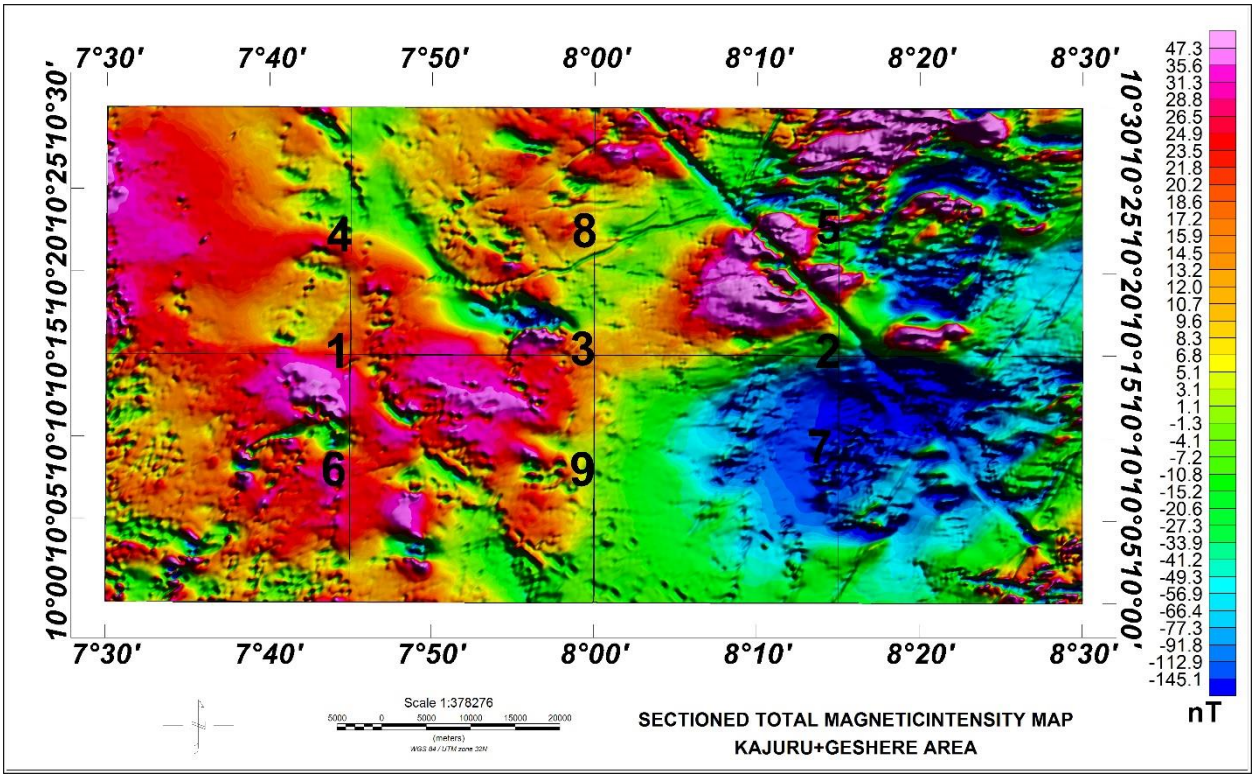

Figure 3: Sectioned Residual Magnetic Intensity map of study area

4.2 Result of Curie Point Depth (CPD) Analysis

Figure (5) in contour mapping, shows the range of Curie point depth variation across the study area. The CPD varies from 12.00 km to 56 km and averages to a value of 30.46 km. Shallow depths were recorded around Wugana, Kajuru, Kasuwan, Magani, New Kwasam towns to the south-western areas and it ranges from 12 to 22 km. High curie depth occurrence of 42 km to 56 km were observed around Unguwar Doka and Kajuma at the

ISSN: 3027-2335 https://fjorae.fudutsinma.edu.ng

north-western and south-eastern part of the study area. The regions delineated with low Curie point depths and high geothermal energy also correspond to fine grained Biotite granite, medium to coarse grained Biotite granite, granite gneiss and porphyritic granite on the geology map (Figure 2).

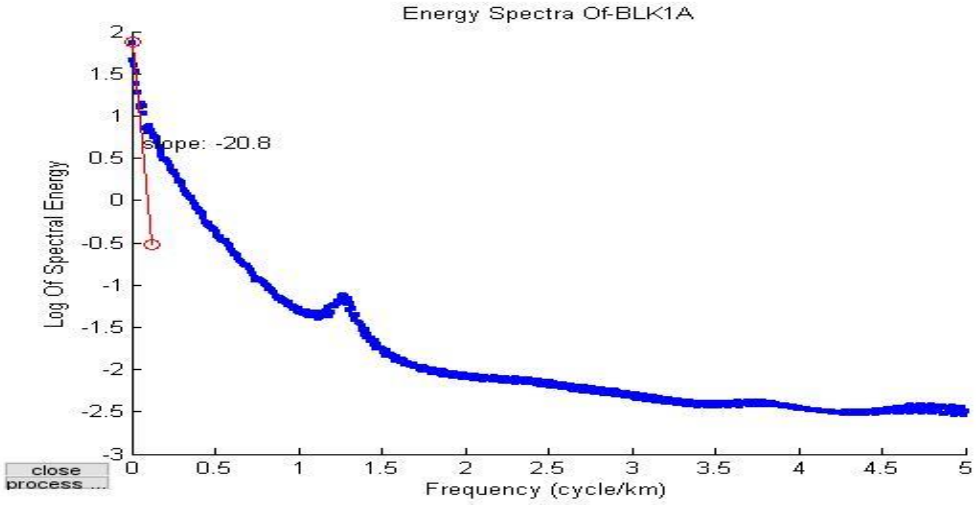

Figure 4: Graph of energy spectrum versus wave number for block 1

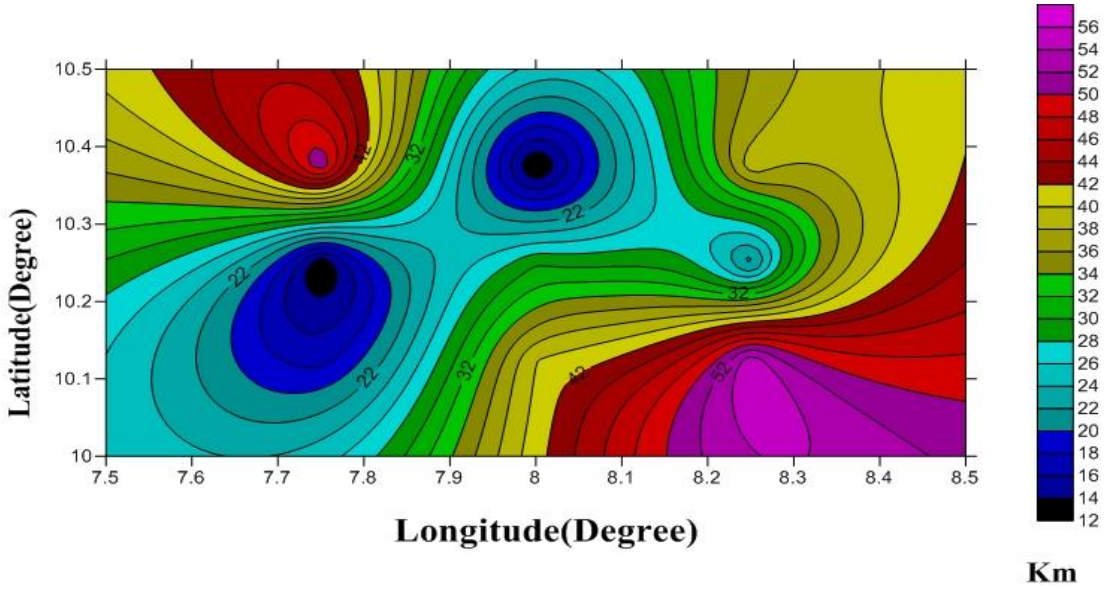

Figure 5: Curie point depth contour map of study area

4.3 Result of the Geothermal Gradients and Heat Flow Analysis

Geothermal gradient in the range of 30 to 50 °C/km Figure (6) was obtained within Wugana, Kajuru, and at the Northern end of the study area, depicting the high geothermal gradient values. Low geothermal gradients were observed at the south-eastern edge, corresponding to the Unguwar Doka area. The heat flow map Figure (7) has values ranges

ISSN: 3027-2335 https://fjorae.fudutsinma.edu.ng

from 30 to 160 mW/m^2 with an average value of 80.60 mW/m^2. Two major regions of study area are noted for high and anomalous values of heat flow, which varies from 105 to 160 mW/m^2. The North-Central regions surrounded by Wugana, Kajuru, New Kwasam and the Western edge of the study area.

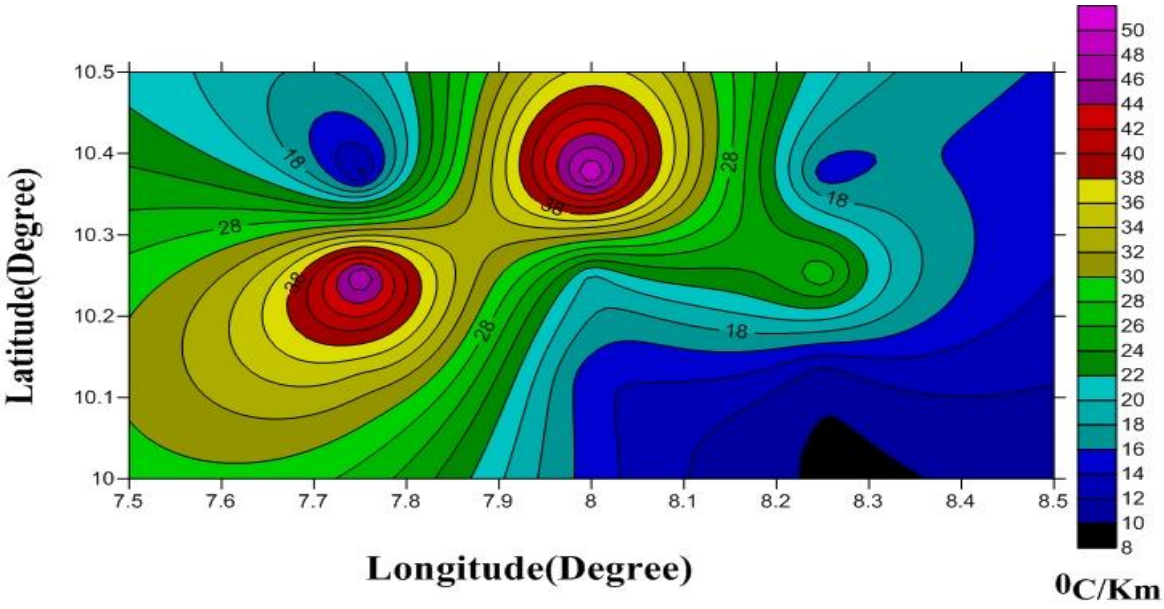

Figure 6: Geothermal gradient contour map of the study area

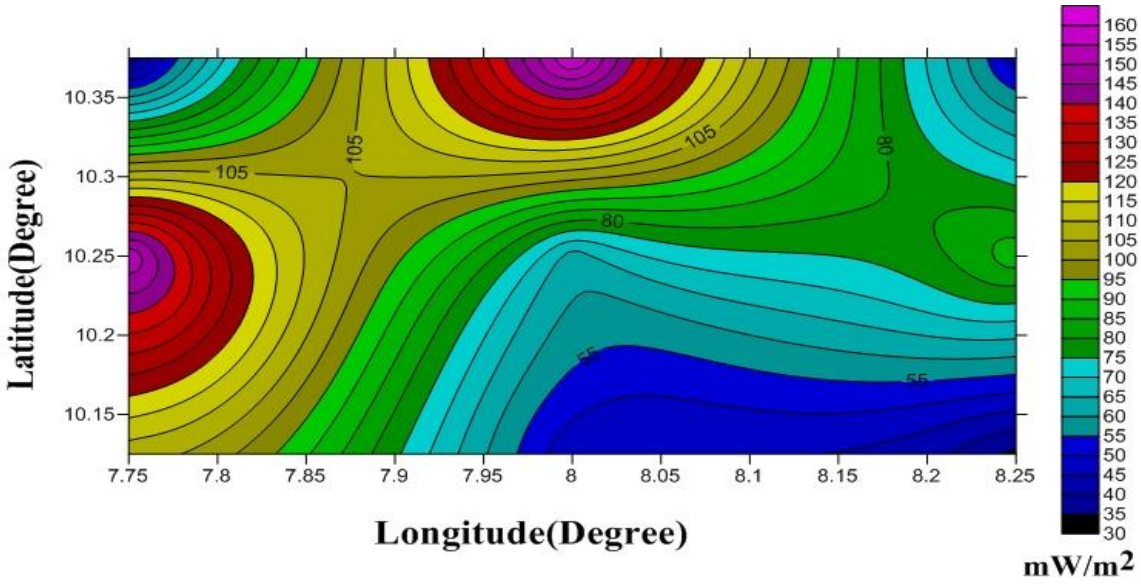

Figure 7: Heat flow contour map of the study area

ISSN: 3027-2335

Table 1: Estimated Curie point depth, geothermal gradient, and heat flow values**.**

Blk	Lon (°E)	Lat (°N)	Depth To Centroid(km)	Depth To Top (km)	Curie point Depth (km)	Heat Flow mW/m²	Geothermal Grad(°C/km)
1	7.75	10.25	14.6	17.2	12.00	154.6666667	48.33333333
2	8.25	10.25	18.9	16.8	21.00	88.38095238	27.61904762
3	8.0	10.25	19.6	9.44	29.76	62.3655914	19.48924731
4	7.75	10.375	29.2	6.72	51.68	35.91331269	11.22291022
5	8.25	10.375	23.6	8.04	39.16	47.39530133	14.81103166
6	7.75	10.125	12.9	8.46	17.34	107.0357555	33.44867359
7	8.25	10.125	32.1	8.8	55.40	33.50180505	10.46931408
8	8.0	10.375	8.44	5.35	11.53	160.971379	50.30355594
9	8.0	10.125	22.5	5.0	40.00	46.4000000	14.50000000

4.4 Result of the Radiometric Analysis

The eTh and eU channel concentrations mappings show high range of values for the radioelements within the study area. This can be related with the geological map Figure (2) showing the regions to be composed mainly of igneous granitic rocks. The total count and equivalent concentration of the radiogenic elements (K, eTh and eU), respectively were fused together to create a ternary image (Figure 8). The result helped in identifying the various rocks that constitute the geology of the study area. The ternary map, is an indication of how the three elements are combined in a colour aggregate which are, red, green, and blue representing potassium, Thorium and uranium respectively. Areas with red colour in the composite map is an indication of strong potassium concentration, while green and blue indicates an area with strong content of equivalent thorium and uranium respectively. Regions with white colour depict high concentration of the three radionuclide elements, these regions correspond to New Kwasam, Kaduna, Idon, and Kasuwan Magani. The study indicates that regions of high concentration of the three radiogenic elements reflect the most probable and viable regions for exploration of geothermal energy.

ISSN: 3027-2335 https://fjorae.fudutsinma.edu.ng

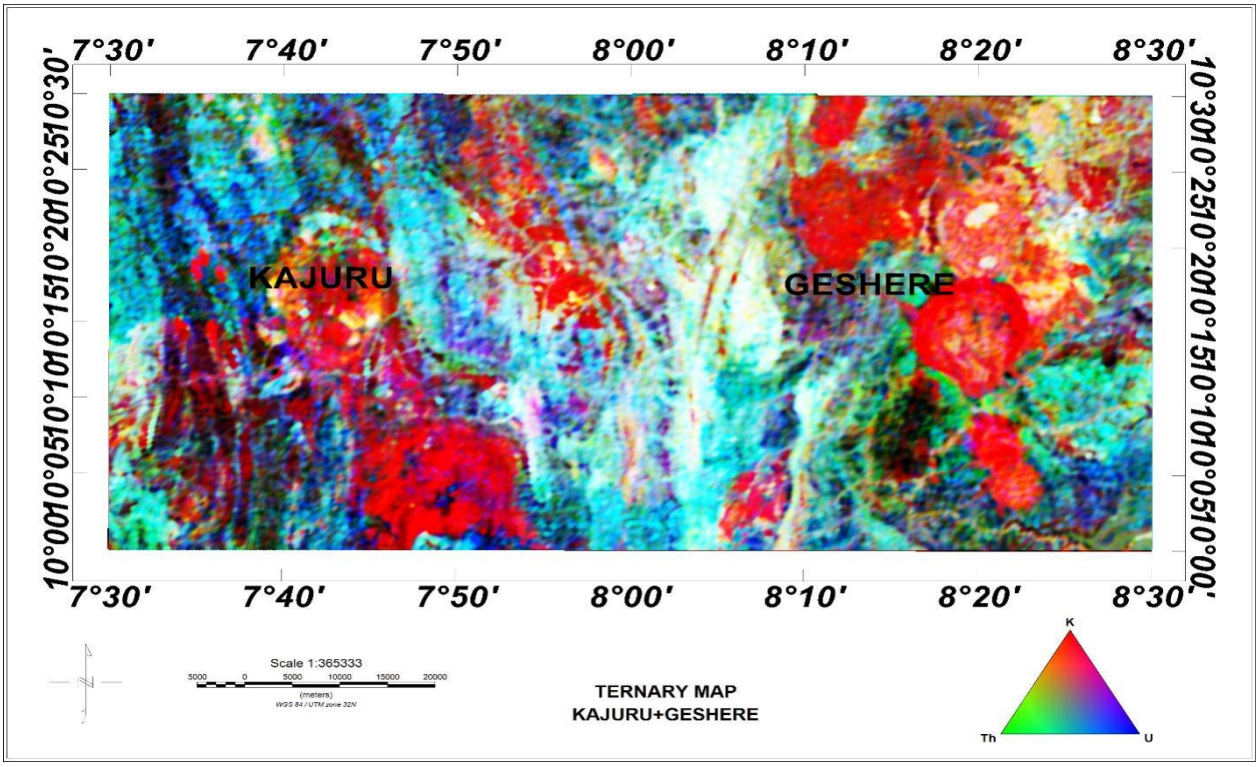

Figure 8: Ternary Map of the Study Area

4.5 Result of the Radioelement Concentration Profiles Analysis

Three main profiles were drawn on the concentration map of each radioelement (K, eTh and eU). The profiles cut across the central points of nine sub sheets used for spectral analysis (Figure 9). The concentration of each radioelement was recorded at the points labelled (P1 to P9) across the study area. The average density of the rock unit hosting the radioelements at each point was also noted and used to calculate the radiogenic heat production at the designated point using equation (8). A summary of estimated RHP values is in table 2.

ISSN: 3027-2335 https://fjorae.fudutsinma.edu.ng

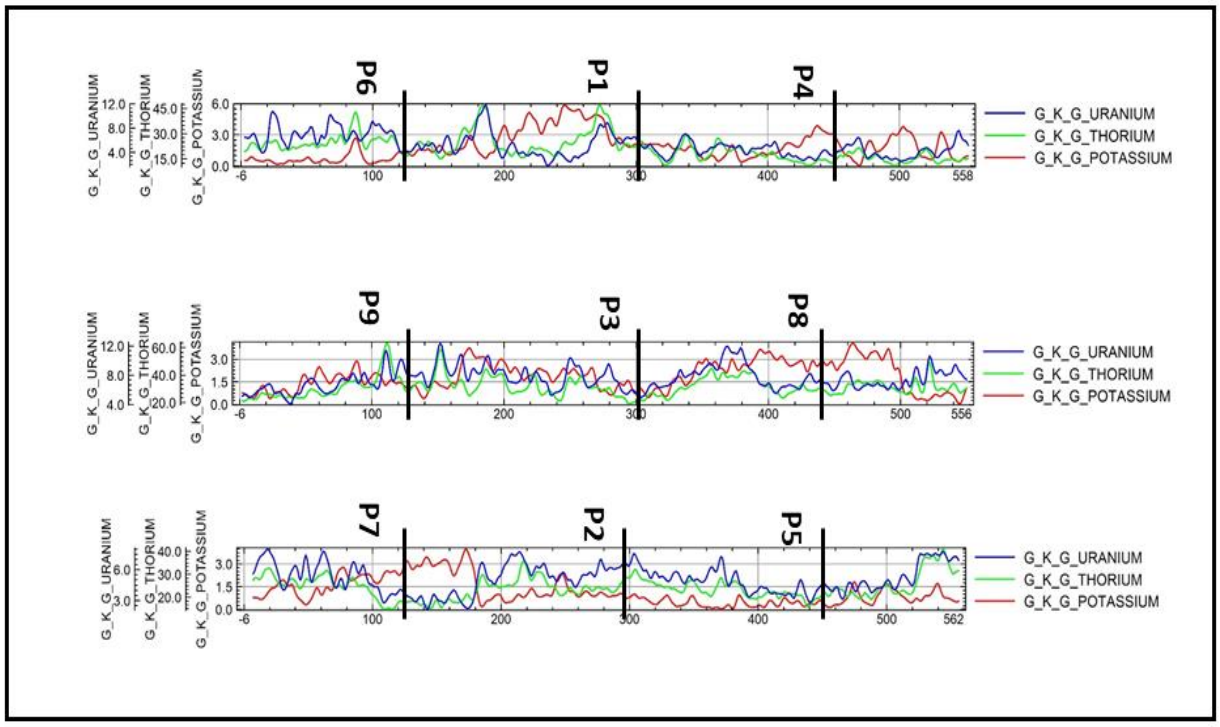

Figure 9: Profiles drawn to record the concentration of the three radioelements (K in red, Th in green and U in blue)

Table 2: Estimated Radiogenic Heat Production of study area

SEC	LON	LAT	K(%)	eTh(ppm)	eU(ppm)	ROCK UNITES	AV. DENSITY(**g/cm³**)	RHP(μW/m³)
1	7.75	10.25	2.0	20.0	8.0	Pophyritic Granite	2.65	3.55948
2	8.25	10.25	0.75	35.0	6.5	Migmatite	2.75	4.237475
3	8.00	10.25	1.25	24.0	6.0	Granite Gnessis	2.65	3.257115
4	7.75	10.375	1.5	22.5	6.0	Porphyritic Granite	2.65	3.17841
5	8.25	10.375	3.2	24.0	4.0	Biotite Granite	2.65	2.932384
6	7.75	10.125	3	17.0	6.0	Migmatite	2.75	3.0547
7	8.25	10.125	0.7	25.0	5.0	Younger Basalt	3.00	2.09236
8	8.00	10.375	1.3	28.0	10.0	Coarse Grain Biotite Granite	2.65	4.542206
9	8.00	10.125	3.0	30.0	8.0	Undifferentiated Schist	2.64	4.31376

4.6 Result of the Radiogenic Heat Production (RHP) Analysis

The radiogenic heat production (Figure 10) reveals the activity of radioelements within their host rocks. The RHP values recorded across the study area range from 2.09 μW/m³ minimum to 4.54 μW/m³ maximum with an average value of 3.46 μW/m³. Peak values

ISSN: 3027-2335 https://fjorae.fudutsinma.edu.ng

were observed in the north and south-central regions, within Wugana, New Kwasan and down to Ron, generally within the intrusive granitic regions. These regions of high RHP also corresponds to regions with high concentration of radio elements as can be seen on Figure (8).

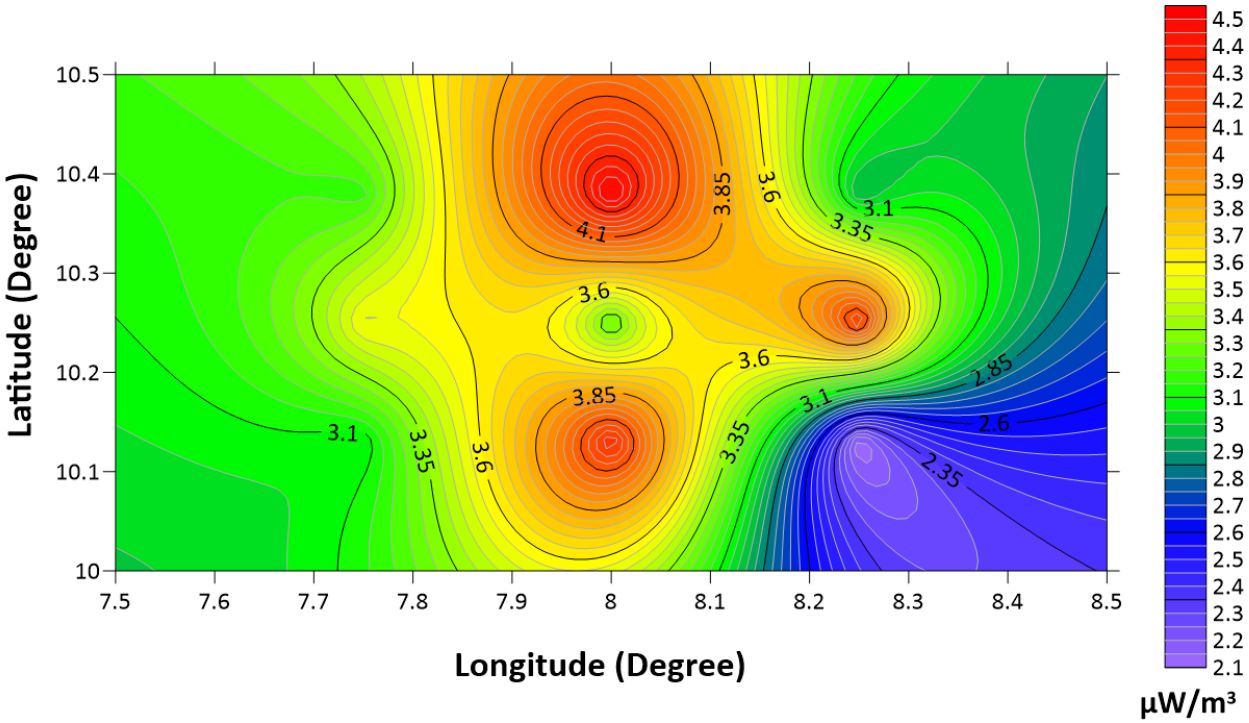

Figure 10: Production of radiogenic heat in the study area.

4.6 Discussion of Results.

The regions observed with the shallowest Curie point depth, high geothermal gradient, and peak values of heat flow are Wugana, Kajuru, and New Kwasam of the study area. The spotted regions show favourable geothermal parameters and could be considered for good potential geothermal sources. Researches have shown that an estimate of the bottom of the magnetized crust represents a direct indicator of the Curie isotherm, variations in the temperature within the crust defines the points of demagnetization and hence the Curie isotherm. (Manea and Manea, 2011; Abdel Zaher 2018a, 2018b; Mono *et al.,* 2018). Hence, the shallow curie depth in a region makes it more viable for harnessing geothermal energy. An inverse variation of Curie point depth with geothermal gradient and heat flow was observed. Regions with decreasing Curie point depth recorded increasing heat flow with geothermal gradient. Generally, values between 80-100 mW/m^2 are good geothermal sources, while values greater than 100 mW/m^2 indicate anomalous conditions (Cull and Conley, 1983; Jessop *et al.,* 1976). The result of this research recorded a peak heat flow value of 160 mW/m^2 which is an indication of an anomalous condition. The range of Curie point and heat flow values obtained in this study also agrees with values earlier gotten from a more regional scale study of geothermal parameters by (Akinyemi and Zui, 2019; Odidi *et al,* 2020). Studies have shown that the average content of Thorium and Uranium

ISSN: 3027-2335 https://fjorae.fudutsinma.edu.ng

within granitic rocks is set at (5 ppm of eU and 15 ppm of eTh), compared to the Earth's crust (averagely 1.8 ppm for U and 7.2 ppm for Th) (Mason & Moore, 1982; Usoif *et al.,* 2015). The maximum range of concentration values observed within the study area (54.39 ppm for eTh and 10.56 ppm for eU) are typically above the usual average and indicates an anomalous condition. The composite radioelement map indicated a high concentration of the three radioelements from the north toward the central regions, a trend that can be related to the observed high radiogenic heat production in the regions. A general convention in geothermal exploration is that values above 4.0 $\mu W/m^3$ are considered high radiogenic heat production and thus a potential economic heat resource (McCay *et al.,* 2014). RHP values of 4.5 $\mu W/m^3$, which is in excess of the recommended threshold, were recorded in the north and central parts of the study area. The geology map in figure 2 indicates the rock types as fine-grained Biotite granite, medium-to-coarse grained Biotite granite, and granite gneiss, which are known to exhibit radioactivity and consequently generate heat in the subsurface. Hence, the high concentration of radionuclides in the area is as a result of the weathering of granite rocks in-situ within the study area.

5. Conclusion

The high resolution aeromagnetic and radiometric data of sheets 145 and 146, covering Kajuru and Geshere within Kaduna State of North Central Nigeria, were analysed using relevant mathematical algorithms such as reduction to equator, Fast Fourier transform, Spectral analysis, and computing the ternary image to access the geothermal and radiogenic heat potentials within the region. Results obtained show that the curie depth has the shallowest depth of 12 km, which coincides with peak geothermal gradient of 50 °C/km and heat flow of 160.9 mW/m^2. Similarly, the radionuclide concentrations for potassium, thorium, and uranium coupled with the average density of the rock lithology gave a maximum estimated radiogenic heat content of 4.5 $\mu W/m^3$ within the same vicinity. It can therefore be concluded that these regions, which falls within Wugana New Kwasan and Ron, can be associated with high geothermal potential. Finally, the high geothermal gradient and heat flow obtained shows a resultant effect of high radio nuclei concentrations within the in-situ basement granitic rocks.

6. Recommendation

The approach in this research work is recommended for other areas where high concentration of radio nuclei is observed for validation.

Conflict of interest

There is no conflict of interest as all contributors are carried along and all materials cited were dully referenced.

References

Abdel Zaher, M., Elbarbary, S., Sultan, S.A., El-Qady, G., Ismail, A., & Takla, E.M. (2018a). Crustal thermal structure of the Farafra oasis, Egypt, based on airborne potential field

ISSN: 3027-2335 https://fjorae.fudutsinma.edu.ng

data. Geothermics 75, pages 220–234. https://doi.org/10.1016/j.geothermics.2018.05.006

Abdel Zaher, M., Saibi, H., Mansour, K., Khalil, A., Soliman, M., (2018b) Geothermal exploration using airborne gravity and magnetic data at Siwa Oasis, Western Desert, Egypt Renewable and Sustainable Energy Reviews Volume 82, Part 3, Pages 3824-3832. https://doi.org/10.1016/j.rser.2017.10.088

Abraham K. M., Lawal A. A (2011) Interpretation of aeromagnetic data for geothermal energy investigation of Ikogosi Warm Spring, Ekiti state, south western Nigeria. International Journal of Scientific research 1: 103-118.

Adetona, A. A., Rafiu, A. A., Aliyu, B. S., John, M. K., & Kwaghhua, I. F. (2024). Estimating the Heat Flow, Geothermal Gradient and Radiogenic Heat within the Young Granites of Jos Plateau North Central Nigeria. Journal of the Earth and Space Physics, 49(4).

Adetona, A. A., Fidelis, I. K., & Shakirat, B. A. (2023). Interpreting the magnetic signatures and radiometric indicators within Kogi State, Nigeria for economic resources. Geosystems and Geoenvironment, 2(2), 100157.

Akinnubi T. D., Adetona A. A. (2018) Investigating the geothermal potential within Benue State, central Nigeria from radiometric and high resolution aeromagnetic data. Journal of Geology and Mining Research. pp.(9)10

Akinyemi, L., & Zui, V. I. (2019). Summary of heat flow studies in Nigeria. Journal of the Belarusian State University. Geography and Geology. No. 2. S. 121-132. https://elib.bsu.by/handle/123456789/240971

Bhattacharyya, B. K., & Leu, L. K. (1975). Spectral analysis of gravity and magnetic anomalies due to two-dimensional structures. Geophysics, 40(6), 993-1013.

Bhattacharyya, B. K., & Leu, L. K. (1977). Spectral analysis of gravity and magnetic anomalies due to rectangular prismatic bodies. Geophysics, 42(1), 41-50.

Blackely, R.J, (1995). Potential theory in gravity and magnetic application. Cambridge University

Brookins, D.G. (1982). Potassium, uranium, thorium radiogenic heat contribution to heat flow in the precambrian and younger silicic rocks of the Zuni and Florida mountains, New Mexico (U.S.A.). Journal of Volcanology and Geothermal Research. Volume 13, Issues 3–4, Pages 189-197. https://doi.org/10.1016/0377-0273(82)90049-X

Bücker, C; Rybach, L (1996). A simple method to determine heat production from gamma-ray logs, Marine and Petroleum Geology 13, 373-375

Chiozzi, P., Pasquale, V., & Verdoya, M. (2003). Heat from radioactive elements in young volcanics by γ-ray spectrometry. Journal of volcanology and geothermal research, 119(1-4), 205-214. https://doi.org/10.1016/S0377-0273(02)00354-2

Cull, J.P, Conley D. (1983). Geothermal Gradients and Heat Flow in Australian sedimentary Basin. Journal of Australian Geology and Geophysics 8: 32-337.

Jessop, A.M., Habart, M.A., Sclater, J.G. (1976). The world heat data collection 1976. Geothermal Services of Canada. Geotherm-ser.50, 251-266

Madu, A., Chinenyeze, J., Aniebonam, A. I., Onuoha M. K. (2015) Density and Magnetic Susceptibility Characterization in the Basement Complex Terrain of NE Kogi State/NW

Benue State of Nigeria. International Journal of Science and Research (IJSR) Volume 5 Issue 12.

Manea, M., and Manea, V.C. (2011). Curie Point depth estimates and correlation with subduction in Mexico. Pure and Applied Geophysics, 168, 1489. https://doi.org/10.1007/s00024-010

Mason, B., & Moore, C. B. (1982). Principles of geochemistry (4th ed.). New York: Wiley.

McCay, A. T., Harley, T. L., Younger, P. L., Sanderson, D. C., & Cresswell, A. J. (2014). Gamma-ray spectrometry in geothermal exploration: State of the art techniques. Energies, 7(8), 4757-4780.

Mock, J. E., Tester, J. W., & Wright, P. M. (1997). Geothermal energy from the earth: its potential impact as an environmentally sustainable resource. Annual review of Energy and the Environment, 22(1), 305-356.

Mono, J. A., Ndougsa-Mbarga, T., Tarek, Y., Ngoh, J. D., & Amougou, O. U. I. O. (2018). Estimation of Curie-point depths, geothermal gradients and near-surface heat flow from spectral analysis of aeromagnetic data in the Loum–Minta area (Centre-East Cameroon). Egyptian journal of petroleum, 27(4), 1291-1299. https://doi.org/10.1016/j.ejpe.2018.07.002

Nwankwo, L. I., & Shehu, A. T. (2015). Evaluation of Curie-point depths, geothermal gradients and near-surface heat flow from high-resolution aeromagnetic (HRAM) data of the entire Sokoto Basin, Nigeria. Journal of Volcanology and Geothermal Research, 305, 45-55.

Obande, G. E., Lawal, K. M., Ahmed, L. A., (2014). Spectral analysis of aeromagnetic data for geothermal investigation of Wikki Warm Spring, north-east Nigeria. Geothermics (50) 85–9. DOI of original article: http://dx.doi.org/10.1016/j.geothermics.2013.08.002.

Odidi, I. G., Abu, M., Nasir, N. (2020). Investigation of Geothermal Energy Potential of Parts of Central and North-Eastern Nigeria Using Spectral Analysis Technique. FUDMA Journal of Sciences (FJS) ISSN online: 2616-1370 ISSN print: 2645 – 2944 Vol. 4 No. 2, pp 627 – 638. DOI: https://d oi.org/10.33003/fjs-2020-0402-248

Olorunsola, K., & Aigbogun, C. (2017). Correlation and mapping of geothermal and radioactive heat production from the Anambra Basin, Nigeria. African Journal of Environmental Science and Technology, 11(10), 517-531.

Okubo, Y., Graf, R. J., Hansen, R. O., Ogawa, K., & Tsu, H. (1985). Curie point depths of the island of Kyushu and surrounding areas, Japan. Geophysics, 50(3), 481-494.

Okubo, Y., Matsushima, J., & Correia, A. (2003). Magnetic spectral analysis in Portugal and its adjacent seas. Physics and Chemistry of the Earth, Parts A/B/C, 28(9-11), 511-519.

Rybach, L. (2010, April). The future of geothermal energy and its challenges. In Proceedings world geothermal congress (Vol. 29).

Rybach, L. (1976). Radioactive heat production: a physical property determined by the chemistry of rocks. The physics and chemistry of minerals and rocks, 309-318.

Salako, K. A., Adetona, A. A., Rafiu, A. A., Alahassan, U. D., Aliyu, A. & Adewumi, T. (2020) Assessment of Geothermal Potential of Parts of Middle Benue Trough, North-East Nigeria. Journal of the Earth and Space Physics, Vol. 45, No. 4. DOI: 10.22059/jesphys.2019.260257.1007017

Spector, A., Grant, F. S. (1970). Statistical models for interpreting aeromagnetic data, Geophysics 35: 293-302.

Stacey, F.O (1977). Physic of the earth John Willey and Sons, New York.

Tanaka, A., Okubo, Y., & Matsubayashi, O. (1999). Curie point depth based on spectrum analysis of the magnetic anomaly data in East and Southeast Asia. Tectonophysics, 306(3-4), 461-470.

Telford, W. M., Geldart, L. P., Sherif, R. E. & Keys, D. A. (1990). Applied Geophysics. Cambridge: Cambridge University Press

Tselentis, G. A. (1991). An attempt to define Curie point depths in Greece from aeromagnetic and heat flow data. pure and applied geophysics, 136, 87-101.

Trifonova, P., Zhelev, Z., Petrova, T., & Bojadgieva, K. (2009). Curie point depths of Bulgarian territory inferred from geomagnetic observations and its correlation with regional thermal structure and seismicity. Tectonophysics, 473(3-4), 362-374.

Uosif, M. A. M., Issa, S. A., & Abd El-Salam, L. M. (2015). Measurement of natural radioactivity in granites and its quartz-bearing gold at El-Fawakhir area (Central Eastern Desert), Egypt. Journal of Radiation Research and Applied Sciences, 8(3), 393-398. https://doi.org/10.1016/j.jrras.2015.02.005

Whitmarsh, R. B., Manatschal, G., & Minshull, T. A. (2001). Evolution of magma-poor continental margins from rifting to seafloor spreading. Nature, 413(6852), 150-154.

Younger, P. L. (2015). Geothermal energy: Delivering on the global potential. Energies, 8(10), 11737-11754.